Chemical signature of magnetotactic bacteria

Matthieu Amor, Vincent Busigny, Mickaël Durand-Dubief, Mickaël Tharaud, Georges Ona-Nguema, Alexandre Gélabert, Edouard Alphandéry, Nicolas F Menguy, Marc F Benedetti, Imène Chebbi, et al.

HAL Id: insu-01446706

https://insu.hal.science/insu-01446706

Submitted on 26 Jan 2017

Chemical signature of magnetotactic bacteria

Matthieu Amor[a,b,1], Vincent Busigny[a], Mickaël Durand-Dubief[c], Mickaël Tharaud[a], Georges Ona-Nguema[b], Alexandre Gélabert[a], Edouard Alphandéry[b,c], Nicolas Menguy[b], Marc F. Benedetti[a], Imène Chebbi[c], and François Guyot[b]

[a]Institut de Physique du Globe de Paris, Sorbonne Paris Cité, Université Paris Diderot, UMR 7154 CNRS, 75238 Paris, France; [b]Institut de Minéralogie, de Physique des Matériaux et de Cosmochimie, Sorbonne Universités, Université Pierre et Marie Curie, UMR 7590 CNRS, Institut de Recherche pour le Développement UMR 206, Museum National d'Histoire Naturelle, 75252 Paris Cedex 05, France; and [c]Nanobactérie SARL, 75016 Paris, France

There are longstanding and ongoing controversies about the abiotic or biological origin of nanocrystals of magnetite. On Earth, magnetotactic bacteria perform biomineralization of intracellular magnetite nanoparticles under a controlled pathway. These bacteria are ubiquitous in modern natural environments. However, their identification in ancient geological material remains challenging. Together with physical and mineralogical properties, the chemical composition of magnetite was proposed as a promising tracer for bacterial magnetofossil identification, but this had never been explored quantitatively and systematically for many trace elements. Here, we determine the incorporation of 34 trace elements in magnetite in both cases of abiotic aqueous precipitation and of production by the magnetotactic bacterium *Magnetospirillum magneticum* strain AMB-1. We show that, in biomagnetite, most elements are at least 100 times less concentrated than in abiotic magnetite and we provide a quantitative pattern of this depletion. Furthermore, we propose a previously unidentified method based on strontium and calcium incorporation to identify magnetite produced by magnetotactic bacteria in the geological record.

magnetotactic bacteria | magnetite | biomineralization | trace element incorporation

Magnetite (Fe_3O_4) is a widespread iron oxide found in geological sedimentary deposits such as banded iron formations, carbonate platforms, or paleosols (1). It can be produced through abiotic or biotic pathways. Magnetotactic bacteria (MTB) and dissimilatory iron-reducing bacteria are known to synthetize magnetite nanoparticles (2).

MTB are magnetite- or greigite (Fe_3S_4)-producing bacteria found in both freshwater and marine environments. They inhabit the oxic–anoxic transition zone under microaerophilic conditions required for their growth. Magnetite or greigite crystals are actively precipitated through biological mechanisms in intracellular organelles called magnetosomes (e.g., refs. 3 and 4). Magnetosomes are assembled in chains inside the cell (Fig. 1) and provide the microorganism with a permanent magnetic dipole. This arrangement allows the bacteria to align themselves along the Earth's geomagnetic field and to reach the optimal position along vertical chemical gradients (5, 6). When the cell dies, magnetosomes may be deposited and trapped into sediments. Magnetite can then be fossilized if the redox conditions are appropriate (1). This mineral may thus be an indirect bacterial fossil. Magnetotactic bacteria have been proposed to represent one of the most ancient biomineralizing organisms (1, 7). Thus, the identification of fossil magnetotactic bacteria, hereafter named bacterial magnetofossils, would provide strong constraints on the evolution of life and of biomineralization over geological times.

Magnetite produced by MTB shows highly controlled crystallographic structure (8). It displays narrow size distributions and is in the magnetic stable single-domain range. Magnetosome chains have remarkable magnetic properties (5, 6, 9), which have been used to identify bacterial magnetofossils in sediments. Although previous studies demonstrated that observations by electron microscopy and/or magnetic measurements could detect bacterial magnetofossils in natural samples (9–13), the chain structure is generally lost during sediment aging owing to degradation of

organic matter assembling magnetosomes (9, 14). This strongly complicates the identification of the bacterial magnetofossils. Moreover, those magnetites undergo variable transformations ranging from isomorphic conversion to maghemite, all the way to crystals that just barely preserve the structural integrity (15). Thus, for bacterial magnetofossil identification in ancient rock samples reliable biosignatures surviving these modifications are still needed for distinguishing biogenic from abiotic magnetite (1, 2).

Geochemical fingerprints can be used as a potential tool for identifying fossilized biominerals (2, 16). For instance, chemical purity has been suggested as a common feature of minerals produced by living organisms (2). The chemical purity of magnetite from MTB has been discussed for many years (e.g., ref. 17). Although not without controversy, it was suggested that low concentrations in minor elements observed in magnetite from Martian meteorite ALH84001 could indicate a biological origin for magnetite (18). This interpretation was supported by abiotic formation of magnetite in the laboratory, leading to high levels of elements other than iron in the crystal products (19, 20), except if initial materials highly depleted in doping elements were used (21). However, the degree of magnetite chemical purity in these previous studies was estimated by energy dispersive x-ray spectroscopy (EDXS) coupled with transmission electron microscopy, which is usually limited to the quantification of relatively elevated elemental concentrations, typically higher than 0.1–1% (22). Moreover, EDXS analyses have been used to evaluate single-element incorporations into magnetite crystals produced by MTB (23–26). These experiments tested only high

Significance

Magnetite precipitates through either abiotic or biotic processes. Magnetotactic bacteria synthesize nanosized magnetite intracellularly and may represent one of the most ancient biomineralizing organisms. Thus, identifying bacterial magnetofossils in ancient sediments remains a key point to constrain life evolution over geological times. Although electron microscopy and magnetic characterizations allow identification of recent bacterial magnetofossils, sediment aging leads to variable dissolution or alteration of magnetite, potentially yielding crystals that barely preserve their structural integrity. Thus, reliable biosignatures surviving such modifications are still needed for distinguishing biogenic from abiotic magnetite. Here, we performed magnetotactic bacteria cultures and laboratory syntheses of abiotic magnetites. We quantified trace element incorporation into both types of magnetite, which allowed us to establish criteria for biomagnetite identification.

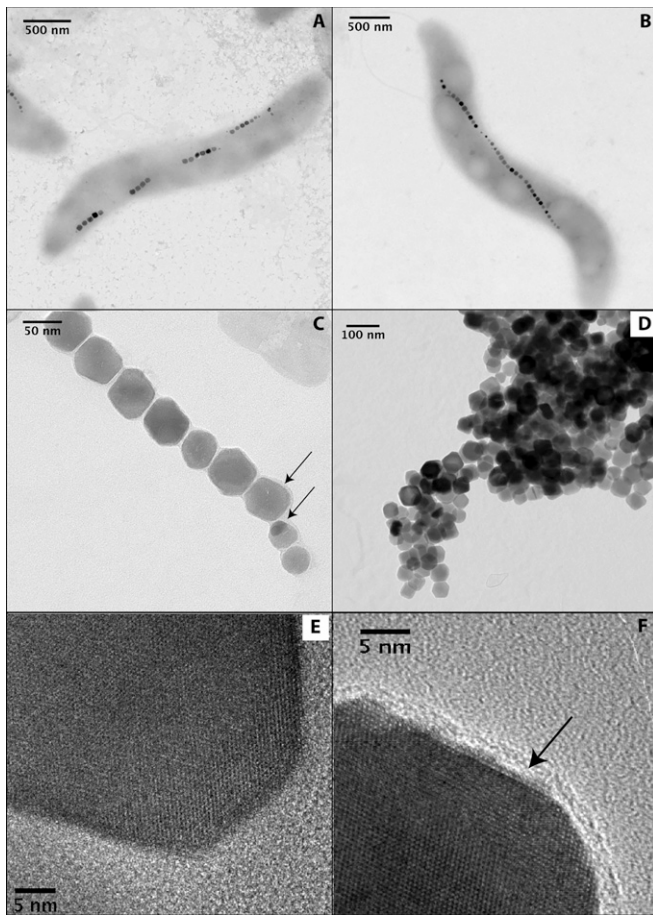EARTH, ATMOSPHERIC, AND PLANETARY SCIENCES

Fig. 1. Transmission electron microscopy images of (*A*) bacteria cultivated in bottles and (*B*) in fermentor, (*C*) extracted chain of magnetosomes, (*D*) magnetosomes treated with SDS-Triton-phenol preparation, (*E*) bacterial magnetite leached with EDTA, and (*F*) untreated magnetosome. Extracted magnetosomes display chain structures assembled by magnetosome membranes and proteins (arrows in *C*). In contrast with magnetite treated with SDS-Triton-phenol (*E*), untreated magnetosomes show traces of organic matter (arrow in *F*). Once treated, magnetite from AMB-1 agglomerated, as shown in *D*. We also observed such agglomeration in abiotic magnetite. Magnetite did not seem to be affected by EDTA leaching.

element concentrations, which may not be representative of natural conditions. A detailed measurement of the low levels of trace elements likely present in trace amounts in magnetite from MTB, together with the knowledge of the concentrations of these elements in the surrounding fluids, thus remain to be established. Indeed, rather than the low or high level of impurity in the magnetite, the important point would be to establish whether differential incorporation of elements exists between biotic and abiotic magnetites. In this work, we thus determined multielement partitioning between aqueous solution and either abiotic magnetite or magnetite from magnetosomes to provide reliable signatures of biological origin.

Abiotic magnetite nanoparticles were synthetized in adapting previous work (27) by mixing Fe^{3+} and Fe^{2+} to which were added 34 trace elements at concentrations of 100 ppb of each element by weight in the solution. This magnetite chemical precipitation is related to an extensive previous literature reporting studies designed for decontamination of wastewaters (e.g., refs. 28 and 29). Our experiments were performed in a glove box to prevent Fe(II) and magnetite oxidation. Biomagnetite was produced from *Magnetospirillum magneticum* strain AMB-1 (ATCC700264) under two different conditions: (*i*) in a fermentor as described in ref. 30 and

(*ii*) in bottles following ATCC recommendations. The initial growth media of the two experiments were different. In contrast with bottle cultures, pH and pO_2 were maintained constant in the fermentor and the medium was continuously homogenized by stirring. These contrasting conditions allow us to evaluate the variability possibly induced by the biosynthesis. In either case, the bacterial growth medium was doped with the same 34 trace elements at 100 ppb each, (i.e., at the same doping level as in the abiotic syntheses). Chains of magnetosomes were extracted from cells with a high-pressure homogenizer. Magnetosome membranes surrounding magnetite were removed using a Triton-SDS-phenol solution heated at 70 °C overnight. Magnetite nanoparticles were leached with ultrapure water and contaminant-free EDTA solution to chelate and remove any element adsorbed on mineral surface (Fig. 1). Abiotic and biotic bottle experiments were carried out in duplicate. Mineralogical characterization (i.e., size, shape, and structure) of the magnetite samples was obtained from X-ray diffraction and transmission electron microscopy (Fig. 1 and Fig. S1). The element concentrations in all experimental products were measured by high-resolution inductively coupled plasma mass spectrometry.

Results and Discussion

Partition Coefficients Between Magnetite and Aqueous Solution. For both biotic and abiotic experiments, elemental partitioning between magnetite and solution is described herein by the partition coefficient normalized to iron:

$$K^{i,Fe} = \frac{C^i_{Mag}/C^i_{Sol}}{C^{Fe}_{Mag}/C^{Fe}_{Sol}}, \quad [1]$$

where i is the element under consideration and C_{Mag} and C_{Sol} are the concentrations in magnetite and residual solution after precipitation, respectively. Partition coefficients are more relevant than the elemental concentrations for characterizing the incorporation of any element in a crystal because they do not depend, in first approximation, on the element concentration in the solution from which the crystal precipitates. In other words, whereas trace element concentrations in magnetite increase when the concentrations in solution increase, the partition coefficient remains constant. Here, the partition coefficient (K) describes the affinity of any chemical element for magnetite, with respect either to the bacterial growth medium or to the solution used for abiotic magnetite precipitation. We normalized the partition coefficient of any element to that of iron. Thus, a K value of 1 indicates that the element shows the same partitioning between magnetite and solution as iron. For $K > 1$, elements are incorporated into magnetite with a stronger affinity than iron, whereas $K < 1$ corresponds to a lower affinity for magnetite relative to iron.

Results show that replicates are consistent between each other in both abiotic and biotic experiments (Fig. S2). We define $K^{i,Fe}_{abiotic}$ and $K^{i,Fe}_{biotic}$ as the average partition coefficients for abiotic magnetite synthesis and bottle and fermentor cultures with AMB-1, respectively. For both abiotic and biotic experiments we calculated the relative standard deviation (RSD) on $K^{i,Fe}_{abiotic}$ and $K^{i,Fe}_{biotic}$ values. Only elements for which the RSD on partition coefficients was lower than 100% were considered for further discussion, but more data are available in Table S1. Partition coefficients of considered elements are reported in Fig. 2. Partition coefficients in abiotic experiments range over seven orders of magnitude, from 10^{-7} to 4. $K^{i,Fe}_{biotic}$ values show narrower variations and lower element incorporations; coefficients cover four orders of magnitude, from 10^{-6} to 10^{-2}. Most elements are therefore more depleted in biogenic magnetite than in abiotic magnetite. Some elements such as strontium show the largest differences between their biotic and abiotic partition coefficients (i.e., four orders of magnitude). Two elements (molybdenum and
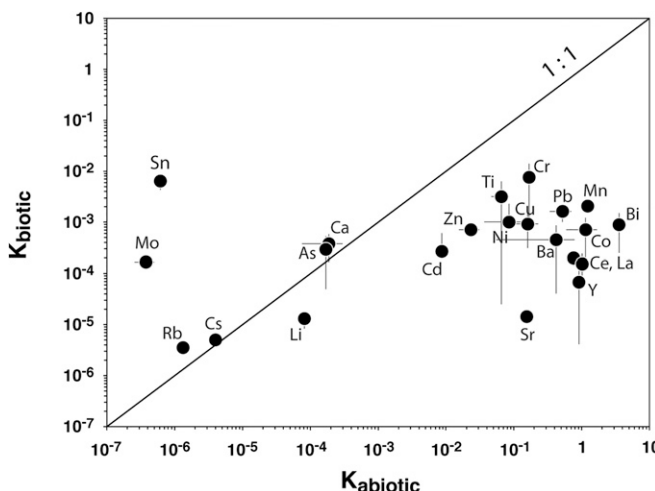
Fig. 2. Element partition coefficients between magnetite and solution for biotic versus abiotic experiments. The partition coefficients are normalized to iron. $K = 1$ indicates a similar behavior of an element relative to iron; $K < 1$ and $K > 1$ correspond to a depletion and an enrichment in the magnetite relative to the exchange of iron between solution and magnetite, respectively. Most elements are depleted in the biogenic magnetite compared with the abiotic magnetite (below the 1:1 thick line). This illustrates the high degree of chemical purity in this biologically controlled mineralization but also shows that the presence of these trace elements in the biomineralization medium is not zero.

tin) show higher concentrations in biogenic magnetite than in magnetite produced in the abiotic synthesis. The good agreement between bottle and fermentor experimental results suggests that partition coefficients are not strongly dependent on the culture conditions.

Chemical Patterns of Biomagnetite. The present data provide a detailed measurement of the very small incorporation of trace elements into magnetite produced by MTB. Even if the concentration of trace elements into magnetite crystals from MTB is low, it is measurable and significantly different from zero. In the present experiments, with the 100-ppb doping level of the aqueous culture medium, the concentrations of most elements measured in biomagnetite ranged between 1 and 10 ppm. With the same doping level in the aqueous medium they typically ranged between 10 and 250 ppm in our abiotic experiments. Our data thus demonstrate that magnetite chemical composition is highly dependent on the precipitation pathway (i.e., abiotic versus biotic). Moreover, different culture conditions of AMB-1 yield similar results of trace element incorporation of the biogenic magnetites, suggesting that the effects of biological variability cannot erase that difference. The main result is thus that, for most elements, partition coefficients between magnetite and the aqueous medium are at least 100 times higher in abiotic magnetite than in biogenic magnetite. In a previous characterization of MTB magnetite chemical composition (17) some elemental concentrations in the magnetite were measured to be as high as 0.4 wt %. However, the composition of the fluid from that previous study is not available, preventing any comparison with the partition coefficients measured here. We tentatively propose that the high concentrations recorded in ref. 17 might be due to an inefficient removal of the magnetosome membrane surrounding magnetites and thus of adsorbed elements at the magnetite surface. Indeed, an extensive literature focusing on wastewater decontamination using abiotic magnetite nanoparticles is based on the optimization of adsorption phenomena on magnetite and other iron oxide or hydroxide phases (28, 29). These studies were aimed at removing as many pollutants as possible by taking advantage of the properties of

magnetite nanoparticles. The high pollutant removal was likely due to surface adsorption as well as incorporation into crystalline structure, and also coprecipitation of separated oxides concentrated in pollutant metals (29). In the case of pollutant removal directly using MTB (26), trace elements were likely adsorbed on the bacterial membrane or complexed with organic matter rather than incorporated into MTB magnetite. In the present work, by strongly cleaning and rinsing the magnetites we studied the incorporation of elements in magnetite.

The differences in partition coefficient patterns between abiotic precipitation and biogenic synthesis can be explained by a biological control of the transfer of chemical elements from the external aqueous solution to magnetosomes. The interior of cells and organelles is usually characterized by elemental concentrations very different from those in the outer medium: elements with important physiological functions, such as iron or calcium, are actively regulated in the cytoplasm (31). The chemical composition of the cell internal medium is thus highly controlled. Elements performing physiological functions or being toxic and too concentrated in the cytoplasm are pumped outward from the cell by efflux transporters located on cell membranes (31). The low concentrations of trace elements observed in magnetite from magnetosomes thus probably reflect their low abundances within the cellular and/or magnetosomal compartments (2). To test this hypothesis, we attempted to analyze trace element content in the cell internal medium, but we were not able to separate the actual internal medium from outer membrane fractions, which were enriched by adsorption and complexation of elements present in the growth medium. If this hypothesis is correct, the chemical composition of magnetites from MTB cultivated in different environments could be translated, using the set of abiotic partition coefficients (Fig. 2), into an estimate of the composition of the actual intracellular medium in which the magnetosomes were synthesized. The magnetite composition, analyzed by following a protocol including severe cleaning and rinsing as in the present study, would then act as a reporter of the chemical composition of the medium from which the magnetosomes grew. In this regard, an interesting but surprising result is that molybdenum and tin display higher partition coefficients in the case of magnetite from MTB than for abiotic magnetite. In biogenic magnetite, molybdenum shows partition coefficients similar to those of zinc, cobalt, or manganese. It is interesting to note that these latter elements are known to be cofactors of metalloenzymes (32) that are essential for bacterial growth and metabolism. Molybdenum is indeed required for nitrate reductase enzymatic activity, which has been reported in AMB-1 and other MTB strains (33, 34). The nitrate reductase reduces nitrate for cell respiration and is also necessary for the magnetite biomineralization in strains MSR-1 and AMB-1 (33, 34).

Implications for Natural Samples. Our data provide a systematic quantification of the degree of purity of biogenic magnetite from MTB, which may thus be used for searching their occurrence in natural environments, in the geological record, and for discussing their possible presence in extraterrestrial materials. In natural rock samples, element concentrations in the ancient fluid phase that were present at the moment of magnetite precipitation are generally not available. Therefore, one has to rely on partition coefficient distributions rather than on raw partition coefficient values. Every single pair of elements could potentially be used to identify magnetite from MTB. As an example, we chose to focus on the strontium/calcium ratio. This ratio differs strongly between magnetite precipitated under abiotic or biotic condition (Fig. 2). Calcium shows a similar partitioning behavior under both conditions ($K_{abiotic}^{Ca,Fe} = 2 \times 10^{-4}$ and $K_{biotic}^{Ca,Fe} = 3 \times 10^{-4}$), whereas strontium is dramatically depleted in biogenic magnetite from MTB ($K_{biotic}^{Sr,Fe} = 1 \times 10^{-5}$) relative to abiogenic magnetite ($K_{abiotic}^{Sr,Fe} = 2 \times 10^{-1}$). We define $K^{Sr,Ca}$ as the partition coefficient of strontium

relative to calcium between magnetite and solution (obtained from the ratio $K^{Sr,Fe}/K^{Ca,Fe}$). $K^{Sr,Ca}$ is independent of iron concentrations in magnetite and solution. From our experimental data, values of $K^{Sr,Ca}$ for abiogenic and biogenic magnetite differ by almost five orders of magnitude, with values at 10^3 and 3×10^{-2}, respectively. Magnetite nanoparticles precipitated by MTB might thus be readily distinguished from their abiotic counterparts if the strontium/calcium ratio of the fluid could be estimated. Magnetite is frequently associated with carbonate minerals in sedimentary and other rocks, including in the Martian meteorite ALH84001 (1, 35). These carbonates may be used as proxies for constraining chemical compositions of fluids that were circulating then. The strontium content in calcium carbonates, such as aragonite and calcite, has been widely studied for this purpose. Strontium/calcium ratios have been measured in various experimental and natural samples, providing a strontium partition coefficient between calcium carbonates and fluids, relative to calcium ($K^{Sr,Ca}_{carbonate}$) (e.g., refs. 36–38). Strontium incorporation into aragonite does not strongly depend on physicochemical conditions, leading to almost constant values of strontium/calcium ratio in aragonite and fluids (36). Strontium incorporation into calcite is more sensitive to chemical conditions of the initial precipitation media (i.e., strontium concentration, salinity, temperature, growth rate), with $K^{Sr,Ca}_{carbonate}$ variations between calcite and fluids being generally in a range from 0.05 to 0.28 (38). Accordingly, strontium/calcium ratio of the fluid can be estimated if buffered by calcium carbonates within a precision of one order of magnitude. Considering the large difference in $K^{Sr,Ca}$ between abiotic and biogenic magnetite from MTB, this precision of strontium/calcium ratio of the fluid is sufficient to determine the possible link between magnetite and MTB by examination of the strontium/calcium ratio in the magnetite. This method could be particularly suitable for ancient terrestrial magnetite samples for which no other criteria can help in establishing their origin (1, 2). Other natural magnetite samples that have been suggested to be from biological origin could be reinvestigated for their chemical composition (18, 39). To our knowledge, trace element data including strontium/calcium ratio in natural magnetite and analyses of cogenetic associated calcium carbonates are not available in the literature, preventing any application of the present method. Future studies should specifically focus on magnetite-bearing limestones to assess the biogenicity of magnetite nanoparticles (7).

Materials and Methods

Abiotic Magnetite Synthesis and Mineralogical Characterization. Magnetite nanoparticles were produced in a glove box (Coy Lab Products), under O_2-free atmosphere, following the protocol described by Ona-Nguema et al. (27). Fe^{3+} and Fe^{2+} ions were mixed in glass flasks to reach the Fe(III)/Fe(II) magnetite stoichiometry. Multielement solution was prepared from inductively coupled plasma mass spectrometry (ICP-MS) standard solutions from Merck Millipore. Initial element concentration was 1,000 ppm for each element. Solutions were diluted to reach a final concentration of 100 ppb in the solution from which magnetite precipitated. Magnetite nanoparticles were precipitated by addition of NaOH to the Fe^{3+}, Fe^{2+}, and multielement solution. Solution was stirred overnight for complete reaction. Nanoparticles were then dried in a desiccator under anoxic conditions. In the present work we focused on elements that are incorporated into the magnetite mineralogical structure and have ensured that elements adsorbed on the mineral surface do not contribute to the magnetite budget. We thus leached magnetite nanoparticles with milli-Q water and a 10 mM EDTA (pH 8) solution following this sequence: (i) water washing, (ii) EDTA leaching for 20 min (handshaking), (iii) water washing, (iv) EDTA leaching for 20 min (handshaking), and (v) two water washings. EDTA was used to remove elements that could be adsorbed on magnetite because of its strong cation-chelation properties and its ability to bind them into stable complexes (40). Between each step magnetite was recovered from supernatant solution using magnets. EDTA solution was prepared with milli-Q water and contaminant-free EDTA powder purchased from Sigma-Aldrich. Magnetite samples were characterized with an X'pert Pro MPD X-ray diffractometer from PANalytical (cobalt anode) and a Jeol J-2100 LaB6 transmission electron microscope

(TEM) operating at 200 kV (Fig. S1). X-ray diffractogram displays typical magnetite peaks. Two replicates were prepared and were consistent between each other (Fig. S2).

Magnetotactic Bacteria Strain Selection. Two strains were available for our culture experiments: *M. magneticum* strain AMB-1 from the ATCC (ATCC700264) and *Magnetospirillum gryphiswaldense* strain MSR-1 from DSMZ (dsm6361). Doping elements toxicity was tested on both strains at five different concentrations: 0 (control) and 1, 10, 100, and 500 ppb. Bacteria cultures for toxicity tests were carried out in standard flask medium (30). Bacterial growth results are presented in Fig. S3.

AMB-1 cultures reached the maximum optical density (OD at 565 nm) of ~0.85 for trace element concentration of 0, 1, 10, and 100 ppb. In contrast, OD was only 0.34 when a concentration of 500 ppb was used. MSR-1 was more affected by doping elements because the growth was altered at 100 ppb: Final OD was 0.37, whereas final OD for lower concentrations was ~0.55. Final OD obtained after growth doped at 500 ppb was only 0.21. Therefore, AMB-1 was selected as the MTB model for our experiments. The bacterial pellet was dark black for doping element concentration of 100 ppb condition, suggesting that a high amount of magnetite was produced. Thus, a concentration of 100 ppb for each element was used for our bacterial cultures. Another benefit of using relatively high concentrations of trace elements was easier and more precise analytical measurements.

Fermentor Culture. AMB-1 was cultivated in a 2-L fermentor (BIOSTAT Aplus; Sartorius) filled with the flask standard medium as described in a previous study (30). Culture conditions were set and maintained at pH 7, temperature 28 °C, pO_2 0.5 mbar, and stirring at 100 rpm. Initial iron concentration was 150 μM Fe(III)-citrate. Doping elements from Merck Millipore ICP-MS standard solutions were added in the culture medium at 100 ppb for each element. We reached a final optical density (OD at 565 nm) of 0.37 after 140 h (Fig. S4). We obtained 1.5 mg of magnetite per liter of culture after extraction and treatment (described below).

Bottle Culture. The strain AMB-1 was cultivated in 2-L glass bottles following instructions from ATCC. Fifty bottles were prepared. The initial pH and temperature were fixed at 6.75 and 30 °C, respectively. The bottle device cannot maintain constant conditions over the time of the culture experiment. Initial iron concentration was 150 μM Fe(III)-citrate. Doping elements from Merck Millipore ICP-MS standard solutions were added to the culture medium at a concentration of 100 ppb for each element. The evolution of OD during the culture is represented in Fig. S4. Each point represents mean OD from four replicates. Maximum OD was reached after 143 h of growth (0.18 ± 0.001). The magnetite production yield was ~0.1 mg per liter of culture after extraction and treatment (described below), about 10 times lower than fermentor culture. Two replicates were prepared and show a good consistency between each other (Fig. S2).

Biogenic Magnetite Extraction and Preparation. Bacteria were collected using a KrosFlo Research Ii*i* tangential filtration system. Chains of magnetosomes were extracted from cultivated bacteria with a pressure homogenizer (EmulsiFlex-C5; Avestin) operating at 100 MPa. The removal of magnetosome membranes is particularly challenging because strong detergents such as pure Triton X-100 or SDS are inefficient (41). Extending the method of a previous study (41), magnetosome membranes were digested in an "in-house" TES buffer and phenol solution. Phenol solution was topped with Tris buffer for storage, preventing any oxidation. TES buffer was prepared by mixing SDS (1 wt %), Triton X-100 (0.5 wt %), EDTA (10 mM, from an EDTA solution stored at pH 8), Tris buffer (10 mM, from a Tris solution stored at pH 7.4), and milli-Q water. After extraction from bacteria, the magnetosome chains were reacted with a solution composed of TES buffer (5 mL) and phenol (5 mL) for 30 min at 70 °C. Magnetite samples were washed in 10 mL of milli-Q water. We repeated this operation twice. They were digested overnight in 10 mL of phenol solution at 70 °C and with 5 mL of TES buffer and 5 mL of phenol solution at 70 °C for 1 h. Finally, all samples were washed 10 times with milli-Q water. Between each step, magnetite samples were recovered with a magnet. Once treated, biogenic magnetite formed aggregates, similar to abiotic magnetite nanoparticles (Fig. 1). No residual magnetosome membranes were observed from transmission electron microscopy (TEM) analyses (Fig. 1 and Fig. S5). In particular, elements tracing organic material, such as phosphorus or nitrogen, were not identified by EDXS analysis.

Before chemical analysis, magnetite nanoparticles were leached with EDTA solution to remove elements adsorbed on mineral surface and rinsed with milli-Q water. The size distribution and shape of magnetite crystals were

monitored to make sure that EDTA and other pretreatments did not dissolve magnetite. High-resolution TEM observations of magnetite nanoparticles were thus carried out after treatment. Crystal surface and edge were undistinguishable in samples before and after treatments. Typical {111}, {110}, and {100} faces were observed in untreated and treated magnetite nanoparticles. Moreover, the apparent surface was undistinguishable in samples before and after treatments, revealing well-defined crystal edges (Fig. 1). Nanoparticle size distributions were also identical, as shown by statistical analysis processed with R programming language (Fig. S6). A detailed description of the statistical analysis is given below.

Magnetite size distribution was established from TEM analyses of magnetite in bacteria, extracted chains of magnetosomes, digested magnetite, and leached magnetite. Magnetosome sizes were measured using image J software. Normal size distributions were confirmed for all samples with a Shapiro–Wilk normality test ($P < 0.001$). ANOVA and Tukey test indicated that the mean size of magnetite in bacteria is statistically lower than that of other samples. This may be due to magnetic recovery of magnetite. Muxworthy and Williams (42) developed the magnetic domain range model for magnetite nanoparticles as a function of the axial ratio, which is defined as the ratio of crystal width over crystal length. Magnetite from AMB-1 possesses an axial ratio close to 1. We infer from this model that AMB-1 magnetite nanoparticles of up to 30 nm in length are superparamagnetic. Superparamagnetic nanoparticles are not magnetically stable at room temperature and may have been lost during magnetic recovery. Therefore, only magnetite nanoparticles with a length of 30 nm or higher were considered for statistical analysis. A new Shapiro–Wilk normality test was significant ($P < 0.001$) and ANOVA analysis confirmed that magnetite mean size did not change after extraction,

purification, and leaching ($P < 0.001$). We conclude that magnetite was not dissolved by EDTA and other pretreatment. Such a statistical analysis was not performed for abiotic magnetite because nanoparticles were strongly agglomerated and their size and shape could not be determined (Fig. S1).

Chemical Analysis. Magnetite samples and solutions after mineral precipitation were dried and dissolved in pure nitric acid (HNO_3) heated at 100 °C. Dissolution experiments were carried out in clean Teflon beakers and in a clean room. Dissolved samples were dried at 100 °C and were dissolved once again at 100 °C in a 0.3 M HNO_3 solution for chemical analyses. Their chemical compositions were assessed using an Element high-resolution ICP mass spectrometer from Thermo Scientific. To ensure that our samples were not contaminated by experimental devices, blanks corresponding to milli-Q water treated like samples were also analyzed. The accuracy of our measurements was checked by analyzing the international standard SLRS-4 (Saint-Laurent River Surface) distributed by the National Research Council–Conseil National de Recherche Canada (43).

1. Kopp RE, Kirschvink JL (2008) The identification and biological interpretation of fossil magnetotactic bacteria. *Earth Sci Rev* 86:42–61.
2. Jimenez-Lopez C, Romanek CS, Bazylinski DA (2010) Magnetite as a prokaryotic biomarker: A review. *J Geophys Res* 115:G00G03.
3. Schüler D (2008) Genetics and cell biology of magnetosome formation in magnetotactic bacteria. *FEMS Microbiol Rev* 32(4):654–672.
4. Komeili A (2012) Molecular mechanisms of compartmentalization and biomineralization in magnetotactic bacteria. *FEMS Microbiol Rev* 36(1):232–255.
5. Bazylinski DA, Frankel RB (2004) Magnetosome formation in prokaryotes. *Nat Rev Microbiol* 2(3):217–230.
6. Faivre D, Schüler D (2008) Magnetotactic bacteria and magnetosomes. *Chem Rev* 108(11):4875–4898.
7. Chang SBR, Kirshcvink JL (1989) Magnetofossils, the magnetization of sediments, and the evolution of magnetite biomineralization. *Annu Rev Earth Planet Sci* 17:169–195.
8. Klumpp S, Faivre D (2012) Interplay of magnetic interactions and active movements in the formation of magnetosome chains. *PLoS ONE* 7(3):e33562.
9. Li J, Wu W, Liu Q, Pan Y (2012) Magnetic anisotropy, magnetostatic interactions and identification of magnetofossils. *Geochem Geophys Geosyst* 13:Q10Z51.
10. Kind J, Gehring AU, Winklhofer M, Hirt AM (2011) Combined use of magnetometry and spectroscopy for identifying magnetofossils in sediments. *Geochem Geophys Geosyst* 12:Q08008.
11. Heslop D, et al. (2013) Quantifying magnetite magnetofossil contributions to sedimentary magnetizations. *Earth Planet Sci Lett* 382:58–65.
12. Kopp RE, et al. (2006) Chains, clumps, and strings: Magnetofossil taphonomy with ferromagnetic resonance spectroscopy. *Earth Planet Sci Lett* 247:10–25.
13. Weiss BP, et al. (2004) Magnetic tests for magnetosome chains in Martian meteorite ALH84001. *Proc Natl Acad Sci USA* 101(22):8281–8284.
14. Kobayashi A, et al. (2006) Experimental observation of magnetosome chain collapse in magnetotactic bacteria: Sedimentological, paleomagnetic, and evolutionary implications. *Earth Planet Sci Lett* 245:538–550.
15. Vali H, Kirshcvink JL (1989) Magnetofossil dissolution in a palaeomagnetically unstable deep-sea sediment. *Nature* 339:203–206.
16. Mandernack KW, Bazylinski DA, Shanks WC, 3rd, Bullen TD (1999) Oxygen and iron isotope studies of magnetite produced by magnetotactic bacteria. *Science* 285(5435):1892–1896.
17. Towe K, Moench TT (1981) Electron-optical characterization of bacterial magnetite. *Earth Planet Sci Lett* 52:213–220.
18. Thomas-Keprta KL, et al. (2000) Elongated prismatic magnetite crystals in ALH84001 carbonate globules: Potential Martian magnetofossils. *Geochim Cosmochim Acta* 64(23):4049–4081.
19. Thomas-Keprta KL, Clemett SJ, McKay DS, Gibson EK, Wentworth SJ (2009) Origins of magnetite nanocrystals in Martian meteorite ALH84001. *Geochim Cosmochim Acta* 73:6631–6677.
20. Jimenez-Lopez C, et al. (2012) Signatures in magnetites formed by (Ca,Mg,Fe) thermal decomposition: Terrestrial and extraterrestrial implications. *Geochim Cosmochim Acta* 87:69–80.
21. Golden DC, et al. (2004) Evidence for exclusively inorganic formation of magnetite in Martian meteorite ALH84001. *Am Mineral* 89:681–695.
22. Eggert F (2006) EDX-Spectra simulation in electron probe microanalysis. Optimization of excitation conditions and detections limits. *Microchim Acta* 155:129–136.
23. Keim CN, Lins U, Farina M (2009) Manganese in biogenic magnetite crystals from magnetotactic bacteria. *FEMS Microbiol Lett* 292(2):250–253.
24. Staniland S, et al. (2008) Controlled cobalt doping of magnetosomes *in vivo*. *Nat Nanotechnol* 3(3):158–162.
25. Tanaka M, et al. (2012) Highest levels of Cu, Mn and Co doped into nanomagnetite magnetosomes through optimized biomineralisation. *J Mater Chem* 22:11919–11921.
26. Arakaki A, Takeyama H, Tanaka T, Matsunaga T (2002) Cadmium recovery by a sulfate-reducing magnetotactic bacterium, Desulfovibrio magneticus RS-1, using magnetic separation. *Appl Biochem Biotechnol* 98-100:833–840.
27. Ona-Nguema G, et al. (2010) XANES evidence for rapid arsenic(III) oxidation at magnetite and ferrihydrite surfaces by dissolved $O_{(2)}$ via $Fe^{(2+)}$-mediated reactions. *Environ Sci Technol* 44(14):5416–5422.
28. Demirel B, Yenigün O, Bekbölet M (1999) Removal of Cu, Ni and Zn from wastewaters by the ferrite process. *Environ Technol* 20:963–970.
29. Barrado E, Prieto F, Castrillejo Y, Medina J (1999) Chemical and electrochemical characterization of lead ferrites produced in the purification of lead-bearing wastewater. *Electrochim Acta* 45:1105–1111.
30. Heyen U, Schüler D (2003) Growth and magnetosome formation by microaerophilic Magnetospirillum strains in an oxygen-controlled fermentor. *Appl Microbiol Biotechnol* 61(5-6):536–544.
31. Naseem R, Holland IB, Jacq A, Wann KT, Campbell AK (2008) pH and monovalent cations regulate cytosolic free Ca^{2+} in E. coli. *Biochim Biophys Acta* 1778(6):1415–1422.
32. Lu Y, Yeung N, Sieracki N, Marshall NM (2009) Design of functional metalloproteins. *Nature* 460(7257):855–862.
33. Li Y, Katzmann E, Borg S, Schüler D (2012) The periplasmic nitrate reductase nap is required for anaerobic growth and involved in redox control of magnetite biomineralization in Magnetospirillum gryphiswaldense. *J Bacteriol* 194(18):4847–4856.
34. Wang K, et al. (2011) Interruption of the denitrification pathway influences cell growth and magnetosome formation in Magnetospirillum magneticum AMB-1. *Lett Appl Microbiol* 53(1):55–62.
35. Thomas-Keprta KL, et al. (2002) Magnetofossils from ancient Mars: A robust biosignature in the martian meteorite ALH84001. *Appl Environ Microbiol* 68(8):3663–3672.
36. Dietzel M, Gussone N, Eisenhauer A (2004) Co-precipitation of Sr^{2+} and Ba^{2+} with aragonite by membrane diffusion of CO_2 between 10 and 50°C. *Chem Geol* 203:139–151.
37. Pingitore NE, Jr, Eastman MP (1986) The coprecipitation of Sr^{2+} with calcite at 25°C and 1 atm. *Geochim Cosmochim Acta* 50:2195–2203.
38. Steuber T, Veizer J (2002) Phanerozoic record of plate tectonic control of seawater chemistry and carbonate sedimentation. *Geology* 30:1123–1126.
39. Schumann D, et al. (2008) Gigantism in unique biogenic magnetite at the Paleocene-Eocene Thermal Maximum. *Proc Natl Acad Sci USA* 105(46):17648–17653.
40. Peters RW (1999) Chelant extraction of heavy metals from contaminated soils. *J Hazard Mater* 66(1-2):151–210.
41. Grünberg K, et al. (2004) Biochemical and proteomic analysis of the magnetosome membrane in Magnetospirillum gryphiswaldense. *Appl Environ Microbiol* 70(2):1040–1050.
42. Muxworthy AR, Williams W (2009) Critical superparamagnetic/single-domain grain sizes in interacting magnetite particles: Implications for magnetosome crystals. *J R Soc Interface* 6(41):1207–1212.
43. Heimburger A, et al. (2012) SLRS-5 elemental concentrations of thirty-three uncertified elements deduced from SLRS-5/SLRS-4 ratios. *Geostand Geoanal Res* 37:77–85.